ACS APPLIED MATERIALS & INTERFACES

Research Article

www.acsami.org

Polyisobutylene-Based pH-Responsive Self-Healing Polymeric Gels

Ujjal Haldar,[†] Kamal Bauri,[†] Ren Li,[‡] Rudolf Faust,[‡] and Priyadarsi De*[,†]

[†]Polymer Research Centre, Department of Chemical Sciences, Indian Institute of Science Education and Research Kolkata, Mohanpur-741246, Nadia, West Bengal India

[‡]Polymer Science Program, Department of Chemistry, University of Massachusetts Lowell, One University Avenue, Lowell, Massachusetts 01854, United States

Supporting Information

ABSTRACT: This work demonstrates the successful application of dynamic covalent chemistry for the construction of self-healing gels from side-chain primary amine leucine pendant diblock copolymers of polyisobutylene (PIB) ((P(H_2N-Leu-HEMA)-*b*-PIB)) in the presence of PIB based dialdehyde functionalized cross-linker (HOC−PIB−CHO) through imine (−HC═N−) bond formation without aiding any external stimuli. Gels were synthesized in 1,4-dioxane at room temperature at varied wt % of gelator concentration, [H_2N]/[CHO] ratios and molecular weight of the block segments. The mechanical property of gels was examined by rheological measurements. We observed higher value of storage modulus (G') than the loss modulus (G'') within the linearity limits of deformation, indicating the rheological behavior in the gel is dominated by an elastic property rather than a viscous property. The G' values significantly depend upon the extent of cross-linking in the gel network. To establish self-healing property of the gels, rheology analysis through step-strain measurements (strain = 0.1 to 200%) at 25 °C was performed. The polymeric gel network shows reversible sol−gel transition for several cycles by adjusting the pH of the medium with the help of hydrochloric acid (HCl) and triethylamine (Et_3N) triggers. FT-IR spectroscopy established formation of imine bonds in the gel network and these gels showed poor swelling behavior in various organic solvents because of the small interstitial porosity, confirmed by field emission-scanning electron microscopy (FE-SEM).

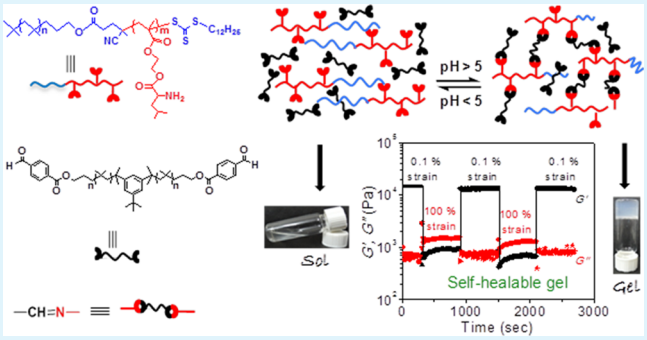

KEYWORDS: *self-healing, amino acids, polyisobutylene, reversible sol−gel transition, storage modulus*

INTRODUCTION

Self-healing is one of the interesting and most fascinating aspect in living organism owing to their self and impulsive ability to heal or repair (fully or partially) the local mechanical damages such as cracks or scratches.[1] These self-healing or self-repairing processes can be achieved without expending any external energy and are sometimes employed via some external stimuli such as pH,[2] temperature,[3] heat,[4] light,[5] or redox.[6] Among all other natural/synthetic materials, polymeric materials offer an extensive area to establish the self-healing or self-repairing properties.[7] Such materials are broadly utilized to prepare safer, fault-tolerant, longer-lasting products and useful in wide range of applications including coatings, electronics, energy, transportation, etc.[8] This self-healing ability in polymeric materials can be developed either through reversible or irreversible mechanistic pathway. In this prospect, reversible mechanism is more promising approach because of their spontaneous ability to repeat the self-healing process for numerous numbers of cycles through noncovalent interaction or dynamic covalent bond formation.[9] Several kinds of reversible molecular interactions play emerging role to design and synthesis of self-healing dynamic gels such as hydrogen bonding, $\pi-\pi$ staking, metal coordination, dynamic covalent bonds, molecular recognition, hydrophobic association, etc.[10]

Dynamic covalent chemistry (DCC) is one of the most promising and reliable approach.[11] Among the various DCC reactions, imine chemistry, disulfide exchange, and boronic acid condensation are the most widely practiced reversible covalent reactions in the self-assembly of molecular architectures.[12] Significant progress has been achieved on the use of Schiff base reactions in the development of polymer chemistry to link structures together.[13] DCC has been applied extensively for making various macromolecular architectures, such as dynamic polymers (dynamers), self-sensing devices, and self-healing substances through some stable and robust bond formation like imine, acylhydrazone via Schiff base reaction.[8,14] Lehn and co-workers employed difunctionalized monomers to prepare dynamic polymer gels through acid sensitive imine bond formation.[15,16] Hydrazone-based self-healable dynamic covalent networks from pentaerythritol tetra(benzohydrazide) and 1,10-

Received: February 10, 2015
Accepted: April 6, 2015
Published: April 6, 2015

DOI: 10.1021/acsami.5b01272
ACS Appl. Mater. Interfaces 2015, 7, 8779−8788

decanediol dibenzaldehyde were prepared and characterized in terms of their swelling, self-healing, and reversibility properties.[17] Deng et al. utilized acylhydrazone bond for the construction of novel dynamic gel, which can be reversibly constructed/broken by adjusting the pH for several cycles and showed interesting self-healing property.[18] A new self-healing hydrogel was developed by the same group with the help of acylhydrazone and disulfide bond exchange reactions in the same systems, can be simultaneously tuned by changing the both pH and redox stimuli.[19] Recently, Zhang et al. designed an inexpensive and simple strategy to prepare dynamic hydrogels using chitosan and dibenzaldehyde-terminated telechelic poly(ethylene gycol) (PEG) moieties.[20] Dynamic covalent exchange and controlled monomer insertion are another effective way to prepare covalently cross-linked gels.[21] Very recently, our group established tryptophan containing pH- and thermoresponsive polymeric gels through acid sensitive imine bond formation using catalytic amount of glacial acetic acid at room temperature.[22] We preferentially chose naturally occurring tryptophan amino acid to construct the dynamic covalent polymeric gels because of their large availability, good biocompatibility and intrinsic fluorescence properties.

On the other hand, polyisobutylene (PIB) shows unique properties such as outstanding thermal and oxidative stability, chemical resistance, excellent damping and barrier property, biocompatibility and biostability.[23] Binder and co-workers reported PIB based self-healing polymeric gels,[24,25] where low glass transition temperature of PIB ensures high chain mobility.[26] The same group also extensively studied self-healing behavior of mono- and bifunctional supramolecular PIBs bearing hydrogen-bonding motifs (such as barbituric acid or a Hamilton wedge).[27−29] Very recently, Faust's group reported rapid and efficient cross-linking of coumarin functionalized PIB triarm star polymers upon irradiation with ultraviolet (UV) light of wavelength (λ_{max}) = 365 nm. Photocleavage was affected by irradiation with UV light at λ_{max} = 254 nm, and the photodimerization/photocleavage cycle was repeated multiple times without the deterioration of the healing ability.[30] Because of the biocompatible nature and diverse properties exhibited by both PIB and side-chain amino acid based polymers, PIB-containing novel diblock copolymers have been synthesized by living cationic polymerization of isobutylene (IB) followed by reversible addition−fragmentation transfer (RAFT) polymerization of side-chain amino acid containing methacrylate monomers in the presence of using PIB macro-chain transfer agents (PIB macro-CTA).[31]

To prepare covalently cross-linked self-healing polymeric gels combining PIB and side-chain amino acid based polymers, in the present study, we reacted side-chain primary amine leucine pendant diblock copolymer of PIB (P(H_2N-Leu-HEMA)-*b*-PIB) in the presence of PIB based dialdehyde functionalized cross-linker (HOC−PIB−CHO) in 1,4-dioxane at room temperature. Free $-NH_2$ moieties in the diblock copolymer formed Schiff base adduct through imine (−CH═N−) bond formation after the reaction with the aldehyde groups in the cross-linker under ambient condition without aiding any external stimuli. We have used PIB-based block copolymer and cross-linker to induce sufficient chain mobility (flexibility) in the gel network. These covalently cross-linked gels can be transformed into sol form in reversible (for several cycles) manner by triggering the pH of the system because of the presence of acid sensitive imine bonds in the gel network. The mechanical property of gels was investigated by varying the gelator concentrations, block length, and $[NH_2]/[CHO]$ ratios. Since the gels were formed from biocompatible amino acids and PIB segments, they are promising candidates for various potential biomedical applications.

EXPERIMENTAL SECTION

Materials. Boc-Leucine (Boc-Leu-OH, 99%), 2-hydroxyethyl methacrylate (HEMA, 97%), *p*-formyl benzoic acid (95%), dicyclohexylcarbodiimide (DCC, 99%), 4-dimethylamino pyridine (DMAP, 99%) were purchased from Sigma-Aldrich and used without any further purification. 2,2′-Azobis (isobutyronitrile) (AIBN, Sigma-Aldrich, 98%) was recrystallized twice from ethanol before use. Trifluoroacetic acid (TFA, 99.5%), triethylamine (Et_3N), and hydrochloric acid (HCl) were obtained from Sisco Research Laboratories Pvt. Ltd., India and used as received. The 4-cyano-4-(dodecylsulfanylthiocarbonylsulfanyl)pentanoic acid (CDP) chain transfer agent (CTA) was synthesized according to the earlier reported procedure.[32] The $PIB_{2k/5k}$ containing macro-CTA ($PIB_{2k/5k}$-CDP)[31] and Boc-leucine methacryloyloxyethyl ester (Boc-Leu-HEMA)[33] were synthesized as reported previously. Two different PIB-CDP macro-CTA having molecular weights 2360 (PIB_{2k}) and 5330 g/mol (PIB_{5k}) were prepared. The solvents such as 1,4-dioxane, hexanes (mixture of isomers), methanol, acetone, ethyl acetate, tetrahydrofuran (THF), dichloromethane (DCM), and *N*,*N*-dimethylformamide (DMF) were purified by standard procedures.[34] NMR solvents, such as $CDCl_3$ (99.8% D) and D_2O (99% D), were purchased from Cambridge Isotope Laboratories, Inc., USA.

Instrumentations. ^{1}H NMR spectra were recorded on a Bruker Avance^{III} 500 spectrometer using tetramethylsilane (TMS) as an internal standard at 25 °C. The FT-IR spectrum was recorded on KBr pellets using a PerkinElmer Spectrum 100 FT-IR spectrometer. Molecular weights and molecular weight distributions (dispersity, *Đ*) were determined by a size exclusion chromatography (SEC) instrument consisting of a Waters 515 HPLC pump, a Waters 2414 refractive index (RI) detector and two columns (Styragel HT4 and Styragel HT3) in THF eluent at 30 °C and the flow rate was 1.0 mL/min. The SEC system was calibrated with polystyrene standards of narrow molecular weight distributions. Thermal stabilities of polymer, cross-linker and dry gel were studied by thermogravimetric analysis (TGA) at 10 °C/min heating rate under N_2 atmosphere by using Mettler Toledo TG/SDTA 851e instrument. The porosity and surface topology of gel samples were examined by field emission-scanning electron microscopy (FE-SEM) on a Carl-Zeiss Sigma instrument. Before the analysis, dry gel samples were coated with gold−palladium alloy for 1 min under high vacuum.

Synthesis of PIB-Bisaldehyde Cross-Linker. First, dihydroxy terminal polyisobutylene (HO−PIB_{2k}−OH) was synthesized by living cationic polymerization (see Supporting Information). Then, HO−PIB_{2k}−OH (2.0 g, 1.0 mmol), 4-formylbenzoic acid (0.45 g, 3.0 mmol), and DMAP (0.025 g, 0.2 mmol) were dissolved in 30 mL of dry THF in a round-bottom flask. The flask was purged with nitrogen and DCC (0.41 g, 2.0 mmol) was added under stirring. The reaction mixture was stirred at room temperature for 28 h, and the white solid was filtered off. The solution was concentrated by using vacuum and precipitated in methanol, followed by repeated (×4) dissolution in hexanes and precipitation in methanol. Finally, it was dried under high vacuum at 35 °C for 12 h to obtain 2.1 g of dialdehyde-functionalized polymer (HOC−PIB_{2k}−CHO).

General Method for the RAFT Polymerization. In a typical example, Boc-Leu-HEMA (1.0 g, 2.91 mmol), PIB_{2k}-CDP (201.2 mg, 0.073 mmol), AIBN (2.4 mg, 0,001 mmol), and 4.0 mL of THF were taken in a 20 mL septum-sealed vial equipped with a small magnetic stir bar. The vial was then purged with dry N_2 for 20 min on an ice-water bath and placed on a preheated reaction block at 60 °C. The polymerization reaction was quenched by cooling the vial in ice-water bath followed by exposure to air. Then, the reaction mixture was diluted with minimum amount of acetone and the polymer was precipitated from cold hexanes. The precipitation process was repeated

DOI: 10.1021/acsami.5b01272
ACS Appl. Mater. Interfaces 2015, 7, 8779−8788

Table 1. RAFT Polymerization of Boc-Leu-HEMA Using $PIB_{2k/5k}$-CDP as a Macro-CTA in THF at 60 °C

polymer	[M]/[CTA]/[I][a]	conversion[b] (%)	$M_{n,theo}$[c] (g/mol)	$M_{n,NMR}$[d] (g/mol)	$M_{n,SEC}$[e] (g/mol)	$Đ$[e]
PIB_{2k}-P(Boc-Leu-HEMA)$_{37}$	40:1:0.2	89	15000	14700	16600	1.32
PIB_{2k}-P(Boc-Leu-HEMA)$_{76}$	80:1:0.2	85	26100	28100	29000	1.40
PIB_{5k}-P(Boc-Leu-HEMA)$_{36}$	40:1:0.2	86	17500	17100	16900	1.34
PIB_{5k}-P(Boc-Leu-HEMA)$_{74}$	80:1:0.2	80	27700	30100	30800	1.32

[a]M = Boc-Leu-HEMA, CTA = $PIB_{2k/5k}$-CDP, and I = AIBN; reaction time = 24 h. [b]Obtained by gravimetric analysis. [c]$M_{n,theo}$ = (([monomer (M)]/[$PIB_{2k/5k}$-CDP macro-CTA] × molecular weight (MW) of monomer × conversion) + (MW of $PIB_{2k/5k}$-CDP macro-CTA)). [d]Calculated from ^{1}H NMR spectroscopy by chain end analysis. [e]Measured by SEC.

Scheme 1. Preparation of $PIB_{2k/5k}$-*b*-P(NH_2-Leu-HEMA) via Boc Group Deprotection, Followed by pH Neutralization at Room Temperature

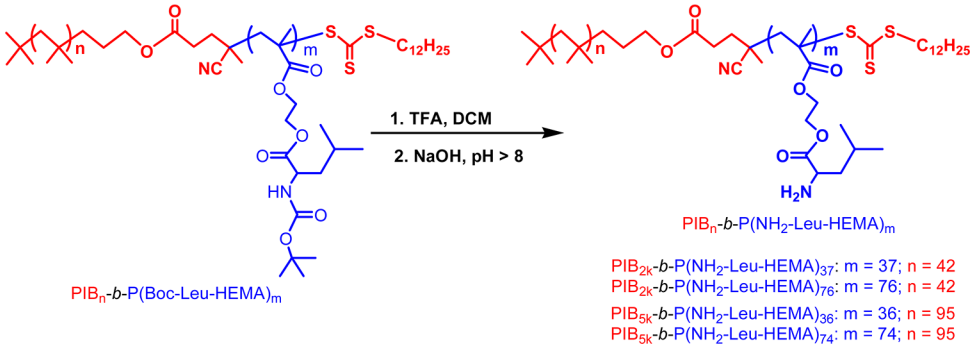

4 times to remove unreacted monomers and macro-CTA. Finally, the resulting product was dried under high vacuum for 12 h at 45 °C.

Preparation of Polymers with Free $-NH_2$ Pendants Through Successive Boc Group Expulsion. Typically, 5.0 mL of TFA was slowly added to the solution containing 1.0 g of Boc protected block copolymer in 5 mL of DCM in a 20 mL glass vial. The solution was stirred for 2 h at room temperature. Then, the polymer was precipitated by addition large volume of cold hexanes, and washed with diethyl ether thrice. Finally, the polymer was dried under high vacuum for 14 h. In the next step, the $-NH_3^+$ containing pendent chains were transformed into free $-NH_2$ groups by the following procedure: 0.7 g of $-NH_3^+$ containing polymer was dissolved in 6.0 mL of deionized (DI) water. After that, 1.0 N NaOH solution was added dropwise into the aqueous polymer solution under stirring until precipitate generated. The precipitate was isolated by centrifugation, washed with DI water thrice, and finally dried under vacuum for 24 h at ambient condition.

Gel Synthesis. Covalently cross-linked gels were prepared using $PIB_{2k/5k}$-*b*-P(NH_2-Leu-HEMA) polymers and PIB containing dialdehyde cross-linker in 1,4-dioxane at room temperature. As an example, 6 wt % (w/v, 120 mg sample/2.0 mL 1,4-dioxane) solution of polymer was prepared in 1,4-dioxane in a 20 mL vial. Appropriate amount of HOC−PIB_{2k}−CHO cross-linker was dissolved in 1,4-dioxane in a 4 mL vial and transferred to the polymer solution. The vial was shaken gently, and gelation happened within 5 min. Similarly, gels were prepared at different wt % of polymer, [NH_2]/[CHO] ratios and molecular weight of $PIB_{2k/5k}$-*b*-P(NH_2-Leu-HEMA) block copolymers.

Purification of Gel. After collecting the crude gel from the reaction vial, it was dialyzed first in hexanes and next in methanol to remove 1,4-dioxane, unreacted HOC−PIB_{2k}−CHO cross-linker and impurities. The dialysis was carried out in a 100 mL beaker and the hexanes or methanol was changed in every 4−8 h for total six times each. Finally, gels were predried at room temperature for 6 h, followed by drying under high vacuum at 45 °C for 2 days. The purified gels were used for FT-IR, TGA, swelling ratio and FE-SEM measurements.

Determination of Equilibrium Swelling Ratio. Measured amount of dry gel (after purification via dialysis) was kept in different solvent (such as hexanes, 1,4-dioxane, DCM, THF, methanol, acetone, DMF) for 48 h to attain the maximum swelling (5 mL solvent in a 20 mL glass vial). Then, the samples were removed from the glass vial and weighed after wiping of the excess surface solvent with a moistened tissue paper. The equilibrium swelling ratio (SR_e) of the swelled gel sample was calculated from the following expression:[35]

$$\text{swelling ratio } (SR_e) = \frac{W_t - W_d}{W_d} \quad (1)$$

where W_t and W_d are, respectively, the weights of the swollen (after 48 h) and dry gels.

Rheology Study. To understand the viscoelastic properties of gels, we have performed rheological experiments on a rheometer (AR-G2, TA Instruments). Gels were prepared in a 20 mL glass vial, aged overnight at room temperature for removing the excess solvents, and finally collected by breaking the glass vial carefully for rheological experiments with the as prepared gels (swollen gels). All the experiments were carried out at 25 °C using 40 mm steel parallel plate with plate gap of 1.0 mm. Storage modulus (G') and loss modulus (G'') of the gels have been recorded in the linear viscoelastic regime at a shear strain of γ = 2% with angular frequency sweep from 0.1 to 100 rad/s.

RESULTS AND DISCUSSION

Synthesis and Characterization of Polymers. Following our previous report,[31] we have polymerized Boc-Leu-HEMA in the presence of $PIB_{2k/5k}$-CDP as macro-CTA and AIBN as radical source in THF at 60 °C. At a fixed AIBN concentration ([$PIB_{2k/5k}$-CDP]/[AIBN] = 1:0.2), two sets of polymerization reactions were carried out by varying the [Boc-Leu-HEMA]/[$PIB_{2k/5k}$-CDP] ratios from 40 to 80 (Table 1). After purification, number-average molecular weights ($M_{n,SEC}$) for these polymers were determined from SEC, which matches nicely with the theoretical number-average molecular weight ($M_{n,theo}$) calculated based on monomer conversion using the formula (Table 1): $M_{n,theo}$ = (([Boc-Leu-HEMA]/[$PIB_{2k/5k}$-CDP macro-CTA] × molecular weight (MW) of Boc-Leu-HEMA × conversion) + (MW of $PIB_{2k/5k}$-CDP macro-CTA)).

Chemical structure of block copolymers was characterized by ^{1}H NMR spectroscopy and all the peaks corresponding to both the blocks were assigned in Supporting Information Figure S1. Comparison of the integration areas of the signals at 2.5 ppm

DOI: 10.1021/acsami.5b01272
ACS Appl. Mater. Interfaces 2015, 7, 8779−8788

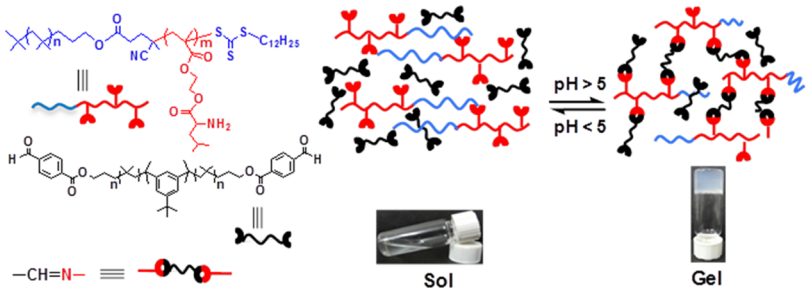

Figure 1. Schematic representation of dynamic covalently cross-linked polymeric gel synthesis from PIB-*b*-P(NH_2-Leu-HEMA) and HOC-PIB-CHO in 1,4-dioxane at room temperature and responsiveness toward pH.

(from the terminal $-CO-CH_2-CH_2-$ protons of PIB-CDP macro-CTA) and 4.1−4.5 ppm (from main chain repeating unit protons due to $-O-CH_2-CH_2-O-$ and chiral proton) allowed calculation of number-average degrees of polymerization ($DP_{n,Boc\text{-}Leu\text{-}HEMA}$) for the P(Boc-Leu-HEMA) block.[31] With these DP_n values (Table 1), we calculated the number-average molecular weight ($M_{n,NMR}$) using the following equation: $M_{n,NMR}$ = [($DP_{n,Boc\text{-}Leu\text{-}HEMA}$ × $M_{Boc\text{-}Leu\text{-}HEMA}$) + molecular weight of $PIB_{2k/5k}$-CDP], where $M_{Boc\text{-}Leu\text{-}HEMA}$ is the molecular weight of Boc-Leu-HEMA monomer. The obtained $M_{n,NMR}$ values also matched nicely with the $M_{n,theo}$ values, and all results are summarized in Table 1. Therefore, well-defined polymers were used for the construction of dynamic covalent gel networks.

In the next stage, deprotection of Boc groups from the $PIB_{2k/5k}$-*b*-P(Boc-Leu-HEMA) block copolymers were carried out by TFA in DCM under ambient condition to obtain water-soluble polymeric salt, $PIB_{2k/5k}$-*b*-P(H_3N^+-Leu-HEMA). We used TFA because of its better solubility profile in organic solvents (DCM in the present study) than the other acids such as HCl and HBr.[36] In the ^{1}H NMR spectrum of deprotected polymer, resonance signal corresponding to the Boc group is absent (Supporting Information Figure S1), thus confirmed successful Boc group deprotection from $PIB_{2k/5k}$-*b*-P(Boc-Leu-HEMA) block copolymers.[37] Then, the side chain repeating unit containing $-NH_3^+$ pendants were transformed to free $-NH_2$ groups by dissolving the polymeric salt into DI water followed by precipitation using 1.0 N NaOH (pH > 8) solution (Scheme 1).[38] Obtained $PIB_{2k/5k}$-*b*-P(NH_2-Leu-HEMA) block copolymers are soluble in various common organic solvents, such as THF, acetone, 1,4-dioxane, DCM, etc., but insoluble in hexanes, toluene, benzene, and water.

Synthesis of Covalently Cross-Linked Gel Using PIB Containing Dialdehyde Cross-Linker. The PIB-bisaldehyde cross-linker (HOC−PIB_{2k}−CHO) was synthesized via straightforward condensation reaction between HO−PIB_{2k}−OH ($M_{n,SEC}$ = 1840 g/mol, $Đ$ = 1.31) and *p*-formyl benzoic acid using DCC as coupling agent and catalytic amount of DMAP. The HOC-PIB_{2k}-CHO was characterized by ^{1}H NMR, FT-IR, and SEC analysis. In the ^{1}H NMR study (Supporting Information Figure S2), the resonance signal corresponding to the methylene proton adjacent to the hydroxyl group of HO−PIB_{2k}−OH appeared at δ = 3.56 ppm, which clearly shifted toward downfield direction (δ = 4.31 ppm) after successful condensation reaction with *p*-formyl benzoic acid. Another important characteristic resonance signal at δ = 10.1 ppm was emerged due to aldehyde protons. No residual resonances from HO−PIB_{2k}−OH were detectable in the resulting HOC−PIB_{2k}−CHO, indicating high degree of functionalization. The integration ratio between methyl protons from PIB backbone at 1.10−0.9 ppm and the terminal aldehyde proton at 10.1 ppm allowed us to determine the $M_{n,NMR}$ as 2220 g/mol (using molecular weight of IB = 56.11 g/mol), which nicely matches with the $M_{n,SEC}$ calculated as 2260 g/mol (with narrow $Đ$ = 1.35). These results clearly demonstrate the high degree of functionality, close to 100%. Supporting Information Figure S3 shows that the SEC trace of HOC−PIB_{2k}−CHO slightly shifted toward higher molecular weight with respect to HO−PIB_{2k}−OH because of the increase in molecular weight after coupling reaction with *p*-formyl benzoic acid. In the FT-IR analysis, a new band appeared at 1726 cm^{-1} in the HOC−PIB_{2k}−CHO due to the ester functional carbonyl group. Also broad peak at 3200−3600 cm^{-1} region in the HO−PIB_{2k}−OH was disappeared in HOC−PIB_{2k}−CHO (Supporting Information Figure S4).

The HOC−PIB_{2k}−CHO was soluble in low polarity solvents like hexanes, toluene, benzene, 1,4-dioxane, THF, etc., because of its long aliphatic saturated carbon chain. For successful gelation reactions, it is important to have common solvent for both the block copolymer and HOC−PIB_{2k}−CHO cross-linker. Although $PIB_{2k/5k}$-*b*-P(NH_2-Leu-HEMA) block copolymers and HOC-PIB_{2k}-CHO cross-linker are soluble in THF and 1,4-dioxane, we decided to carry out gelation reactions in 1,4-dioxane because of its high boiling point and less volatility at room temperature in comparison to THF. Initially, 6 wt % (w/v) of PIB_{2k}-*b*-P(NH_2-Leu-HEMA)$_{37}$ and HOC-PIB_{2k}-CHO were dissolved in 1.0 mL of 1,4-dioxane in two separate vials. Then, the homogeneous solution of HOC−PIB_{2k}−CHO was added to the PIB_{2k}-*b*-P(NH_2-Leu-HEMA)$_{37}$ solution at room temperature, and shaken gently. A sharp increase in viscosity was clearly noticed within 2 min and finally gelation was completed within 5 min (Figure 1). During the gel synthesis in 1,4-dioxane at room temperature, we varied wt % of PIB_{2k}-*b*-P(NH_2-Leu-HEMA)$_{37}$ at constant [H_2N]/[CHO] = 1 ratio (G11 to G15 in Table 2), [H_2N]/[CHO] ratios at 6 wt % of PIB_{2k}-*b*-P(NH_2-Leu-HEMA)$_{37}$ (G13, G16 and G17 in Table 2) and PIB_{5k}-*b*-P(NH_2-Leu-HEMA)$_{36}$ (G21, G22, and G23 in Table 2). Also, molecular weights of amino acid blocks were varied at constant wt % of polymer and [H_2N]/[CHO] ratio (Table 2): G13 and G33 for PIB_{2k} and G21 and G44 for PIB_{5k}. Table 2 summarizes the gelation times for all the gels, which were obtained by visual observation. Generally, in the literature acid or base catalysts are added to adjust the pH of the reaction medium and effective gelation reaction at lower time-scale for the construction of self-healable gels via imine bond formation.[22,39] However, in the present system gels were prepared in very short period of times without addition of external stimuli at room temperature. That could have

DOI: 10.1021/acsami.5b01272
ACS Appl. Mater. Interfaces 2015, 7, 8779−8788

Table 2. Dynamic Gel Formation from the Schiff-Base Reaction between $PIB_{2k/5k}$-*b*-P(NH_2-Leu-HEMA) with HOC−PIB_{2k}−CHO in 1,4-Dioxane at Room Temperature[a]

gel	polymer	$[NH_2]/[CHO]$ ratio[b]	wt% of polymer[c]	$DP_{n,Boc\text{-}Leu\text{-}HEMA}$	gelation time (min)
G11	PIB_{2k}-*b*-P(NH_2-Leu-HEMA)$_{37}$	1.0	2	37	10
G12	PIB_{2k}-*b*-P(NH_2-Leu-HEMA)$_{37}$	1.0	4	37	7
G13	PIB_{2k}-*b*-P(NH_2-Leu-HEMA)$_{37}$	1.0	6	37	5
G14	PIB_{2k}-*b*-P(NH_2-Leu-HEMA)$_{37}$	1.0	8	37	3
G15	PIB_{2k}-*b*-P(NH_2-Leu-HEMA)$_{37}$	1.0	10	37	2
G16	PIB_{2k}-*b*-P(NH_2-Leu-HEMA)$_{37}$	0.5	6	37	11
G17	PIB_{2k}-*b*-P(NH_2-Leu-HEMA)$_{37}$	0.3	6	37	13
G21	PIB_{5k}-*b*-P(NH_2-Leu-HEMA)$_{36}$	1.0	6	36	15
G22	PIB_{5k}-*b*-P(NH_2-Leu-HEMA)$_{36}$	0.5	6	36	21
G23	PIB_{5k}-*b*-P(NH_2-Leu-HEMA)$_{36}$	0.3	6	36	26
G33	PIB_{2k}-*b*-P(NH_2-Leu-HEMA)$_{76}$	1.0	6	76	4
G44	PIB_{5k}-*b*-P(NH_2-Leu-HEMA)$_{74}$	1.0	6	74	3

[a]Every formulation in Table 2 was prepared using a total of 2 mL of 1,4-dioxane. [b]$M_{n,NMR}$ values were used to formulate the $[NH_2]/[CHO]$ ratios. [c]wt % of PIB-*b*-P(NH_2-Leu-HEMA) in solution.

happened most probably because of the following two reasons: first, the transition pH values of the block copolymer were between 6.2 and 6.7 (Supporting Information Figure S5), where imine bonds are stable. Second, flexible nature and high chain mobility of the PIB segment (both in the block copolymer and cross-linker) helps to attain every possible orientations to make Schiff-base adduct formation with the multi amino pendent polymeric chains under ambient condition.

Characterization of Gels. To ensure the imine bond formation after the reaction between PIB_{2k}-*b*-P(NH_2-Leu-HEMA) and HOC-PIB_{2k}-CHO, we recorded their FT-IR spectra along with the dried cross-linked G13 gel. Figure 2A clearly depicts that the absorption band appeared at 1701 cm^{-1} because of the aldehyde groups present on the HOC−PIB_{2k}−CHO is completely disappeared in the dry gel. Furthermore, a new band originated at 1641 cm^{-1} in the FT-IR spectrum of gel. This peak is assigned to the C═N vibrations of imines,[40] thus demonstrating imine bond formation after the gelation reaction. Note that the absence of aldehyde peak at 1701 cm^{-1} in the gel ensures us complete condensation (or removal during the purification) of the HOC−PIB_{2k}−CHO cross-linker after the gelation process.

Thermal stability of PIB_{2k}-*b*-P(NH_2-Leu-HEMA)$_{37}$, HOC−PIB_{2k}−CHO and corresponding dry covalently cross-linked gel was investigated by TGA analysis (Figure 2B). Two-step degradation was observed for PIB_{2k}-*b*-P(Boc-Leu-HEMA)$_{37}$. The first stage decomposition at 205 °C (onset degradation temperature where the horizontal and tangent intersect) to 260 °C could be due to the loss of side chain repeating units (ester groups), and afterward at 330−350 °C residual chains degraded.[41] The HOC-PIB_{2k}-CHO showed single step degradation at 395 °C. Although covalently cross-linked gel showed single stage degradation with 50% weight loss at 320 °C, decompositions started at ∼150 °C because of the side-chain cleavage.

Rheological Behavior of Covalently Cross-Linked Gel. To investigate the viscoelastic behavior of the covalently cross-linked gels, we performed oscillatory rheological measurements at stress sweep and frequency sweep modes at room temperature. Preliminarily, we performed G' and G'' versus % strain of G13 gel sample (Table 2) to determine the linear viscoelastic regime. It was observed that, the gel can bear approximately 40% strain at the angular frequency of 0.1 rad/s (Figure 3A). Hence, we performed all other frequency sweep measurements at a constant strain of 2.0%, which is well below the deformation range in the vicoelastic regime. In all the cases, G' value was higher than the G'' and it never intersects each other throughout the applied frequency range, which implies the elastic nature and characteristic features of gels.

From the frequency sweep measurements, our interest was to study the effect of gelator concentration, block lengths, and $[NH_2]/[CHO]$ ratios variation on the G' values of gels. Figure 3B depicts the change of G' with variation of gelator concentration at a constant $[H_2N]/[CHO]$ = 1 ratio (G11−G15 in Table 2). It was observed that with increasing the gelator concentration from 2 to 6 wt %, the G' value increased because of higher availability of the two reactive functional groups in the system (less gelation time at higher wt % of polymer). But the effect was not prominent at higher gelator

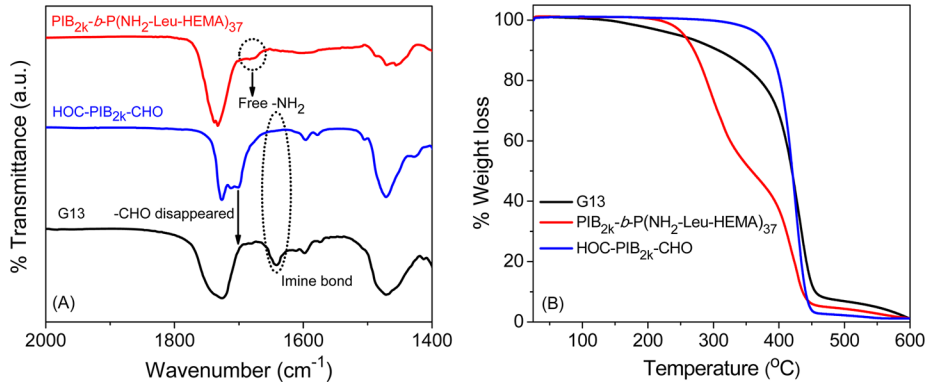

Figure 2. (A) FT-IR spectra of PIB_{2k}-*b*-P(NH_2-Leu-HEMA)$_{37}$, HOC−PIB_{2k}−CHO, and cross-linked G13 gel in Table 1. (B) TGA curves of PIB_{2k}-*b*-P(NH_2-Leu-HEMA)$_{37}$, HOC-PIB_{2k}-CHO, and dry G13 gel in Table 1

DOI: 10.1021/acsami.5b01272
ACS Appl. Mater. Interfaces 2015, 7, 8779−8788

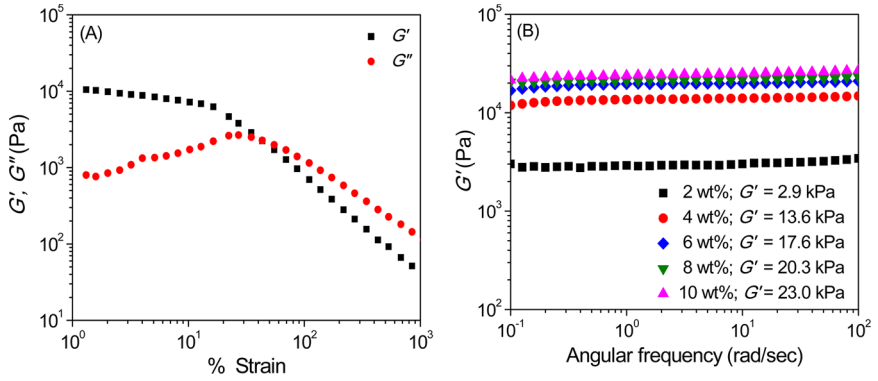

Figure 3. Rheological properties of gels obtained from the cross-linking reaction between PIB_{2k}-*b*-$P(NH_2$-Leu-HEMA$)_{37}$ and HOC-PIB_{2k}-CHO in 1,4-dioxane at room temperature: (A) strain sweep measurement at a constant frequency (0.1 rad/s) of 1 Hz for G13 gel in Table 1 and (B) G' versus angular frequency at a constant stain (2%) for the gels prepared at various wt % polymer solutions (G11-G15 in Table 1).

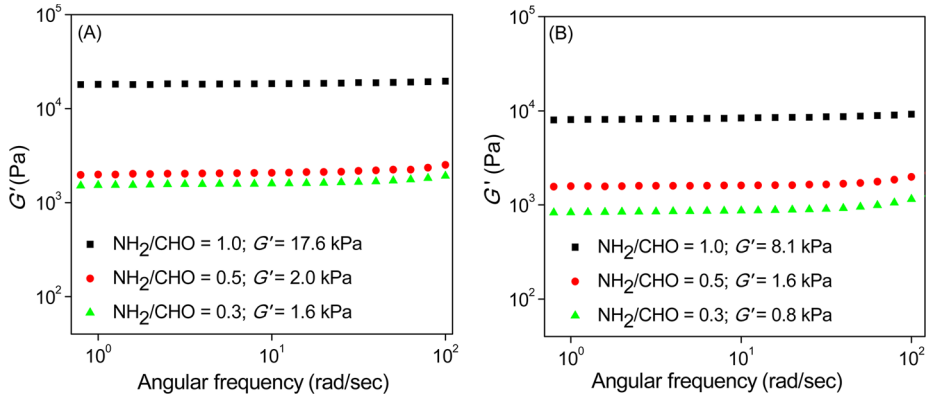

Figure 4. G' versus angular frequency at a constant stain (2%) for the gels obtained from PIB_{2k}-*b*-$P(NH_2$-Leu-HEMA$)_{37}$ (A) and PIB_{5k}-*b*-$P(NH_2$-Leu-HEMA$)_{36}$ (B) at different $[NH_2]/[CHO]$ ratios at a constant 6 wt % (w/v) gelator concentration.

concentrations, that is, from 6 to 10 wt %. This result indicates saturation of imine bond formation after a certain wt % of the gelator concentration.

Next, effect of $[NH_2]/[CHO]$ ratios during gel formation was studied. Figure 4 displays the G' as a function of angular frequency for the gels obtained from PIB_{2k}-*b*-$P(NH_2$-Leu-HEMA$)_{37}$ (Figure 4A, gels G13, G16, and G17 in Table 2) and PIB_{5k}-*b*-$P(NH_2$-Leu-HEMA$)_{36}$ (Figure 4B, gels G21, G22 and G23 in Table 2) at different $[NH_2]/[CHO]$ ratios at a constant 6 wt % (w/v) gelator concentration. It was observed that the value of G' increased with the increase of $[NH_2]/[CHO]$ ratio from 0.3 to 0.5 to 1 in the polymer network. This is probably due to the enhanced cross-linking among the polymeric chains at maximum NH_2/CHO ratio.[22] As expected, the angular frequency independent G' along with a plateau storage modulus were obtained for both the series.

It was observed (comparing G' values in Figure 4A and Figure 4B) that the G' of the gel achieved from the PIB_{2k}-*b*-$P(NH_2$-Leu-HEMA$)_{37}$ showed higher value in comparison to the gel obtained from PIB_{5k}-*b*-$P(NH_2$-Leu-HEMA$)_{36}$. This happened because of the main chain $PIB_{2k/5k}$ block, since the same cross-linker was used during the gel formation and $DP_{n,\text{Boc-Leu-HEMA}}$ is almost same in the above two block copolymers. The PIB_{5k} block is comparatively less flexible with lower chain mobility than the PIB_{2k} segment, and as a consequence the stiffness of the gel displayed lower value in the gels prepared from PIB_{5k}-*b*-$P(NH_2$-Leu-HEMA$)_{36}$. Also, note that the gel formed from PIB_{2k} has a higher effective cross-link density.

The G' values also can be varied by changing the molecular weight of the block segments (Figure 5). At a constant PIB_{2k}

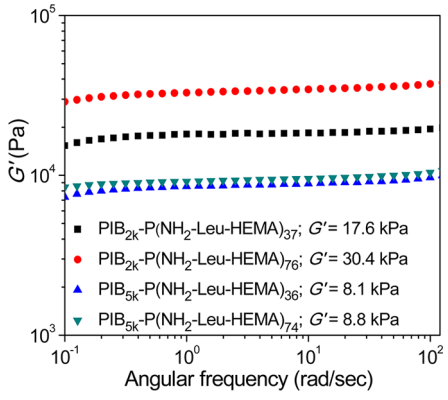

Figure 5. G' versus angular frequency (2% strain) of polymeric gels with varying the block length. Gels were prepared in 1,4-dioxane at room temperature at constant 6 wt % of polymer and $[H_2N]/[CHO]$ = 1 ratio (Table 1, G13 and G33 for PIB_{2k}, and G21 and G44 for PIB_{5k}).

length, the obtained G' of PIB_{2k}-*b*-$P(NH_2$-Leu-HEMA$)_{37}$ polymeric gel is slightly lower than the gel obtained from PIB_{2k}-*b*-$P(NH_2$-Leu-HEMA$)_{76}$ (G13 and G33 in Table 2). This happened due to larger number of reactive amine pendent chains in the later polymer, which enhanced the cross-linking density and made stiff gel network. Similar kind of trend was

DOI: 10.1021/acsami.5b01272
ACS Appl. Mater. Interfaces 2015, 7, 8779−8788

followed by other gels at constant PIB_{5k} segment, which were formed from PIB_{5k}-*b*-P(NH_2-Leu-HEMA)$_{36}$ and PIB_{5k}-*b*-P-(NH_2-Leu-HEMA)$_{74}$ (G21 and G44 in Table 2). However, difference of G' values was not so much prominent in the case of G21 and G44, which suggests that main chain PIB block plays some effective role to reduce the toughness of the gel.

Thixotropic gel has ability to disintegrate to solution or quasi-liquid state under some external stimuli and can regain their original shape after removal of the applied stimuli.[42,43] This process can be continued for several numbers of cycles via breaking and reconstructing the gels. To establish thixotropic property in the present gels, we have performed rheological step-strain measurements under varying strain at room temperature (Figure 6). Initially, the gel was treated under

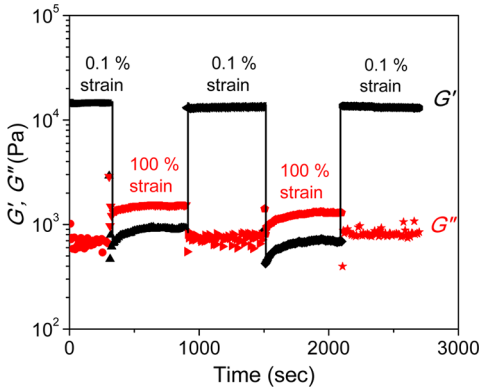

Figure 6. Variation of G' and G'' during the continuous step strain measurement at alternate 0.1% and 100% strain (frequency = 0.1 rad/s) with time scale.

very low strain (0.1%), which is reasonably below the deformation limit, as a result G' (14650 Pa) showed higher value than G'' (760 Pa). But when we increased the strain (100%, kept for few minutes), the gel was collapsed to form sol/quasi liquid state and lost its mechanical stability, confirmed by the complete inversion of the G' and G'' value, where G'' displayed higher value than G'. After the high strain was released, the sol state again transformed into semisolid state and quickly regained its mechanical strength and we found almost 96% recovery under the low strain of 0.1%. This self-recovery process was continued for 3 cycles under varying strain to establish the self-healing property.[44] Also, we varied the strain from 100% to 200% under a constant frequency (Supporting Information Figure S6). Here too, we found almost 95% recovery in a very short time. The shortened recovery time can be attributed to the main chain flexible PIB segments and the PIB end functionalized aldehyde cross-linker, which can produce enormous flexibility for effective cross-linking reaction. Nevertheless, self-healing happens via dynamic imine bond formation through successive dissociation and recombination of primary amine and aldehyde functionalities, which clearly indicates that some functional groups remain free for further chemical interactions for initiation of the self-healing process.

We kept the G13 gel on a petridish for 2 months in open atmosphere. The gel became hard due to evaporation of the exterior and interior solvents. After 2 months it showed almost 2.4-fold higher G' (43.0 kPa) compared to the measurement with the freshly prepared gel after 18 h (G' = 17.6 kPa). The higher G' is attributed to the higher cross-linking reaction between the unreacted primary anime and aldehyde functionalities during the extended period of time. Also, the gel was able to bear higher strain (113%) before its deformation, shown in Supporting Information Figure S7. The above gel regained its softness after swelling in 1,4-dioxane.

pH Responsiveness of Gels. Reversible dynamic sol−gel phase transition property was investigated as a function of the pH of the reaction medium. The gel was prepared in 1,4-dioxane using 6 wt % (w/v) of PIB_{2k}-*b*-P(NH_2-Leu-HEMA)$_{37}$ and appropriate amount of PIB containing dialdehyde cross-linker at [NH_2]/[CHO] = 0.5 at room temperature without adding any external acid or base. The pH of the corresponding solution was measured as 6.7 and the gel was formed within 5 min. Then, approximately 30 μL of concentrated HCl was added into the polymeric gel, and within 15 min the gel was transformed into solution state due to the breakage of imine bond in acidic environment. Next, exactly equivalent amount of Et_3N was added into the polymeric solution and gently stirred. The pH of the solution was measured as 5.5 and after sometime sol was transformed into the gel phase. Addition of Et_3N base transformed the $-NH_3^+$ groups to the deprotonated $-NH_2$ groups, which leads to the formation of imine bond with the aldehydes cross-linker. This sol−gel transition process was carried out up to seven times to emphasize its dynamic nature (Figure 7A). During the transition of first cycle to seventh

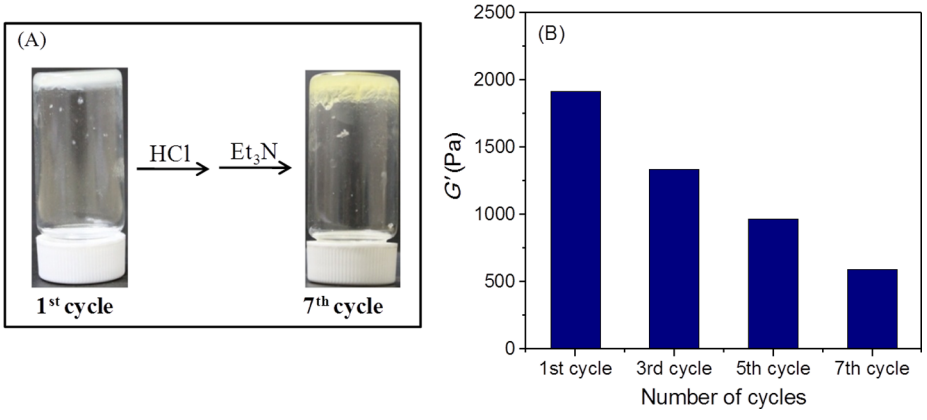

Figure 7. (A) Pictorial representation of the gel after first and seventh sol−gel transition process, where the initial gel was prepared from the mixture of 6 wt % (w/v) of PIB_{2k}-*b*-P(NH_2-Leu-HEMA)$_{37}$ and HOC-PIB_{2k}-CHO at [NH_2]/[CHO] = 1 in 1,4-dioxane at room temperature. (B) Variation of G' of the gel after different sol−gel transition cycles.

DOI: 10.1021/acsami.5b01272
ACS Appl. Mater. Interfaces 2015, 7, 8779−8788

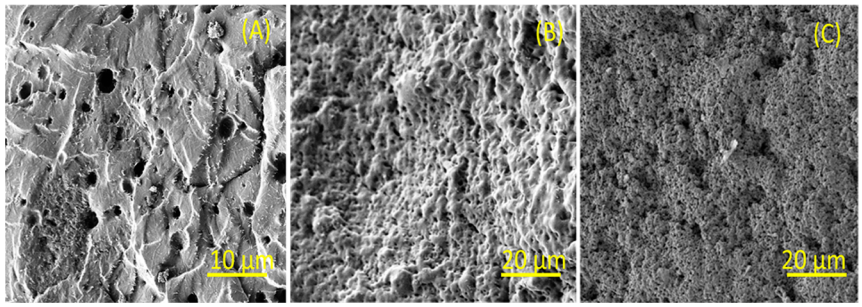

Figure 8. FE-SEM images of covalently cross-linked gels prepared by the condensation of PIB_{2k}-*b*-$P(NH_2$-Leu-HEMA$)_{37}$ (6 wt %) with HOC−PIB_{2k}−CHO in 1,4-dioxane at room temperature using different $[NH_2]/[CHO]$ ratios: (A) 0.3 (B) 0.5, and (C) 1.0.

cycles, increased amount of HCl after each cycle was required to decompose the gel and gelation time increased after every cycle (5 min in the first cycle and 40 h at the seventh cycle). After the first sol−gel transition cycle, a precipitate of Et_3N.HCl appeared in the system and as a result the clarity and transparency of the gels reduced slightly. To check the effect of sol−gel transition process on the mechanical properties of gels, G' was determined for the gels after each acid−base treatment cycles (Figure 7B and Supporting Information Figure S8). It was interesting to observe substantial decrease in G' after each cycle, probably because of the presence of Et_3N·HCl salt and enhanced volume of the system with the addition of HCl and Et_3N after each cycle. The Et_3N·HCl salt probably perturbs the gelation process and impose heterogeneity into the gel matrix as a result the resulting gel became weak.

To investigate the interior morphology of synthesized covalently cross-linked gels, FE-SEM images were recorded (Figure 8). The morphology of the cross-linked gel depends on cross-link density, concentration of polymer in solution during the gelation reaction and the solvent in which gels were prepared.[45] It was interesting to observe that, with varying $[NH_2]/[CHO]$ ratios (1 to 0.5 to 0.3) the porosity in the gel network increased because of lesser cross-linking between two reactive functional groups. However, sizes of the pores are relatively smaller than the conventional chemically cross-linked gels,[46] perhaps because of the highly cross-linked interconnected microdomain formed here in a very short period of times during the course of gelation reaction.

Solvent Uptake Capacity of Gels. The swelling ability of the covalently cross-linked gels depends on several factors, such as the nature of the substituents (hydrophilic/hydrophobic), solvent polarity and gelation mechanism. Since FE-SEM studies showed porous structures, solvent uptake capacity of gels were studied in different organic medium. The SR_e values of the dried G33 polymeric gels were determined in various organic solvents of different polarities ranging from nonpolar (hexanes) to highly polar solvents (DMF). The swelling ratio is maximum in case of THF (SR_e = 2.1) (Supporting Information Figure S9) and least in methanol (SR_e =0.04). The SR_e values in other solvents are summarized in Supporting Information Figure S10. Note that we did not find any correlation of SR_e values with the solvent polarity, most probably due the diverse nature of the solubility of PIB and $P(NH_2$-Leu-HEMA) segments. Nevertheless, poor solvent uptake capacity was observed due to the extremely interconnected networks occurred during gelation reaction, as a consequence the size of the pores were reduced, which was clearly reflected in FE-SEM images.

CONCLUSIONS

In summary, we have successfully synthesized amino acid based covalently cross-linked self-healing polymeric gel network from $P(H_2$N-Leu-HEMA)-*b*-PIB block copolymer in the presence of a HOC−PIB_{2k}−CHO cross-linker with the help of dynamic covalent chemistry through Schiff-base linkage at room temperature. These Schiff-base linkages can be broken and again regenerated for several cycles in reversible manner by adjusting the pH of the system through successive addition of acid or base, although substantial decrease in G' was observed after each cycle. Mechanical strength of the dynamic gels were increased with increasing the gelator concentration in solutions, $[NH_2]/[CHO]$ ratio and $DP_{n,\text{Boc-Leu-HEMA}}$ in the block copolymer at a constant PIB block length. However, G' values decreased with the increased length of the PIB block at a constant $DP_{n,\text{Boc-Leu-HEMA}}$ of the block copolymer due to the lower chain mobility of PIB_{5k} than the PIB_{2k} segment. These gels displayed self-healing property at room temperature as strain sweep experiments at both low (0.1%) and high strain (200%) indicated the thixotropic property of the gel network. Poor swelling ability of the gels indicated highly inter connected networks formed during gelation reaction, which was also reflected from its low interior porosity by FE-SEM images. Such pH responsive dynamic covalently cross-linked gels carrying reasonable mechanical stability will create a new insight in the development of smart soft materials for the applications in organ repair and pH triggered delivery of biologically relevant materials.[47,48]

ASSOCIATED CONTENT

Supporting Information

Synthesis of HO−PIB−OH, ^{1}H NMR spectra of block copolymers, HO−PIB−OH and HOC−PIB_{2k}−CHO, SEC traces of HO−PIB−OH and HOC−PIB_{2k}−CHO, variation of G' at $[NH_2]/[CHO]$ = 0.5, continuous step strain measurement, swelling images of gel in THF and swelling ratio studies in various organic solvents. This material is available free of charge via the Internet at http://pubs.acs.org.

AUTHOR INFORMATION

Corresponding Author

*E-mail: p_de@iiserkol.ac.in.

Notes

The authors declare no competing financial interest.

ACKNOWLEDGMENTS

This work was supported by the Department of Science and Technology (DST), India [Project No.: SR/S1/OC-51/2010].

DOI: 10.1021/acsami.5b01272
ACS Appl. Mater. Interfaces 2015, 7, 8779−8788

U. Haldar and K. Bauri acknowledge Council of Scientific and Industrial Research (CSIR), Government of India, for their fellowships.

REFERENCES

(1) Murphy, E. B.; Wudl, F. The World of Smart Healable Materials. *Prog. Polym. Sci.* **2010**, *35*, 223−251.
(2) Yoshida, R. Self-Oscillating Gels Driven by the Belousov−Zhabotinsky Reaction as Novel Smart Materials. *Adv. Mater.* **2010**, *22*, 3463−3483.
(3) Wei, Q.; Wang, J.; Shen, X.; Zhang, X. A.; Sun, J. Z.; Qin, A.; Tang, B. Z. Self-Healing Hyperbranched Poly(aroyltriazole)s. *Sci. Rep.* **2013**, *3*, 1093−1098.
(4) Jeong, B.; Kim, S. W.; Bae, Y. H. Thermosensitive Sol−Gel Reversible Hydrogels. *Adv. Drug Delivery Rev.* **2002**, *54*, 37−51.
(5) Murata, K.; Aoki, M.; Suzuki, T.; Harada, T.; Kawabata, H.; Komori, T.; Ohseto, F.; Ueda, K.; Shinkai, S. Thermal and Light Control of the Sol−Gel Phase Transition in Cholesterol-Based Organic Gels. Novel Helical Aggregation Modes As Detected by Circular Dichroism and Electron Microscopic Observation. *J. Am. Chem. Soc.* **1994**, *116*, 6664−6676.
(6) Nakahata, M.; Takashima, Y.; Yamaguchi, H.; Harada, A. Redox-Responsive Self-Healing Materials Formed From Host−Guest Polymers. *Nat. Commun.* **2011**, *2*, 511−516.
(7) Fischer, H. Self-Repairing Material Systems—A Dream or a Reality? *Nat. Sci.* **2010**, *2*, 873−901.
(8) Lehn, J.-M. Dynamers: Dynamic Molecular and Supramolecular Polymers. *Prog. Polym. Sci.* **2005**, *30*, 814−831.
(9) Syrett, J. A.; Becer, C. R.; Haddleton, D. M. Self-Healing and Self-Mendable Polymers. *Polym. Chem.* **2010**, *1*, 978−987.
(10) Wei, Z.; Yang, J. H.; Zhou, J.; Xu, F.; Zrınyi, M.; Dussault, P. H.; Osada, Y.; Chen, Y. M. Self-Healing Gels Based on Constitutional Dynamic Chemistry and Their Potential Applications. *Chem. Soc. Rev.* **2014**, *43*, 8114−8131.
(11) Rowan, S. J.; Cantrill, S. J.; Cousins, G. R. L.; Sanders, J. K. M.; Stoddart, J. F. Dynamic Covalent Chemistry. *Angew. Chem., Int. Ed.* **2002**, *41*, 898−952.
(12) Jin, Y.; Wang, Q.; Taynton, P.; Zhang, W. Dynamic Covalent Chemistry Approaches Toward Macrocycles, Molecular Cages, and Polymers. *Acc. Chem. Res.* **2014**, *47*, 1575−1586.
(13) Xin, Y.; Yuan, J. Schiff's Base as a Stimuli-Responsive Linker in Polymer Chemistry. *Polym. Chem.* **2012**, *3*, 3045−3055.
(14) Lehn, J.-M. From Supramolecular Chemistry Towards Constitutional Dynamic Chemistry and Adaptive Chemistry. *Chem. Soc. Rev.* **2007**, *36*, 151−160.
(15) Fujii, S.; Lehn, J.-M. Structural and Functional Evolution of a Library of Constitutional Dynamic Polymers Driven by Alkali Metal Ion Recognition. *Angew. Chem., Int. Ed.* **2009**, *48*, 7635−7638.
(16) Folmer-Andersen, J. F.; Lehn, J.-M. Constitutional Adaptation of Dynamic Polymers: Hydrophobically Driven Sequence Selection in Dynamic Covalent Polyacylhydrazones. *Angew. Chem., Int. Ed.* **2009**, *48*, 7664−7667.
(17) Apostolides, D. E.; Patrickios, C. S.; Leontidis, E.; Kushnir, M.; Wesdemiotis, C. Synthesis and Characterization of Reversible and Self-Healable Networks Based on Acylhydrazone Groups. *Polym. Int.* **2014**, *63*, 1558−1565.
(18) Deng, G.; Tang, C.; Li, F.; Jiang, H.; Chen, Y. Covalent Cross-Linked Polymer Gels with Reversible Sol−Gel Transition and Self-Healing Properties. *Macromolecules* **2010**, *43*, 1191−1194.
(19) Deng, G.; Li, F.; Yu, H.; Liu, F.; Liu, C.; Sun, W.; Jiang, H.; Chen, Y. Dynamic Hydrogels with an Environmental Adaptive Self-Healing Ability and Dual Responsive Sol−Gel Transitions. *ACS Macro Lett.* **2012**, *1*, 275−279.
(20) Zhang, Y. L.; Tao, L.; Li, S. X.; Wei, Y. Synthesis of Multiresponsive and Dynamic Chitosan-Based Hydrogels for Controlled Release of Bioactive Molecules. *Biomacromolecules* **2011**, *12*, 2894−2901.
(21) Amamoto, Y.; Kikuchi, M.; Masunaga, H.; Sasaki, S.; Otsuka, H.; Takahara, A. Reorganizable Chemical Polymer Gels Based on Dynamic Covalent Exchange and Controlled Monomer Insertion. *Macromolecules* **2009**, *42*, 8733−8738.
(22) Roy, S. G.; Bauri, K.; Pal, S.; De, P. Tryptophan Containing Covalently Cross-Linked Polymeric Gels with Fluorescence and pH-Induced Reversible Sol−Gel Transition Properties. *Polym. Chem.* **2014**, *5*, 3624−3633.
(23) Kenedy, J. P.; Ivan, B. *Designed Polymers by Carboncationic Macromolecular Engineering: Theory and Practice*; Hancer Gardner, Cincinnati, OH, 1992.
(24) Döhler, D.; Michael, P.; Binder, W. H. Autocatalysis in the Room Temperature Copper(I)-Catalyzed Alkyne−Azide "Click" Cycloaddition of Multivalent Poly(Acrylate)s and Poly(Isobutylene)s. *Macromolecules* **2012**, *45*, 3335−3345.
(25) Döhler, D.; Zare, P.; Binder, W. H. Hyperbranched Polyisobutylenes for Self-Healing Polymers. *Polym. Chem.* **2014**, *5*, 992−1000.
(26) Herbst, F.; Döhler, D.; Michael, P.; Binder, W. H. Self-Healing Polymers *via* Supramolecular Forces. *Macromol. Rapid Commun.* **2013**, *34*, 203−220.
(27) Herbst, F.; Seiffert, S.; Binder, W. H. Dynamic Supramolecular Poly(Isobutylene)s for Self-Healing Materials. *Polym. Chem.* **2012**, *3*, 3084−3092.
(28) Binder, W. H.; Sachsenhofer, R. "Click" Chemistry in Polymer and Materials Science. *Macromol. Rapid Commun.* **2007**, *28*, 15−54.
(29) Binder, W. H.; Sachsenhofer, R. "Click" Chemistry in Polymer and Material Science: An Update. *Macromol. Rapid Commun.* **2008**, *29*, 952−981.
(30) Banerjee, S.; Tripathy, R.; Cozzens, D.; Nagy, T.; Keki, S.; Zsuga, M.; Faust, R. Photoinduced Smart, Self-Healing Polymer Sealant for Photovoltaics. *ACS Appl. Mater. Interfaces* **2015**, *7*, 2064−2072.
(31) Bauri, K.; De, P.; Shah, P. N.; Li, R.; Faust, R. Polyisobutylene-Based Helical Block Copolymers with pH-Responsive Cationic Side-Chain Amino Acid Moieties by Tandem Living Polymerizations. *Macromolecules* **2013**, *46*, 5861−5870.
(32) Moad, G.; Chong, Y. K.; Postma, A.; Rizzardo, E.; Thang, S. H. Advances in RAFT Polymerization: The Synthesis of Polymers with Defined End-Groups. *Polymer* **2005**, *46*, 8458−8468.
(33) Bauri, K.; Roy, S. G.; Pant, S.; De, P. Controlled Synthesis of Amino Acid-Based pH-Responsive Chiral Polymers and Self-Assembly of Their Block Copolymers. *Langmuir* **2013**, *29*, 2764−2774.
(34) Furniss, B. S.; Hannaford, A. J.; Smith, P. W. G.; Tatchell, A. R. *Vogel's Textbook of Practical Organic Chemistry*; Longman Scientific & Technical Copublished in the United States with John Wiley & Sons, Inc: New York, 1989.
(35) Yoon, J. A.; Chakicherla, G.; Gil, R. R.; Kowalewski, T.; Matyjaszewski, K. Comparison of the Thermoresponsive Deswelling Kinetics of Poly(2-(2-Methoxyethoxy)ethyl methacrylate) Hydrogels Prepared by ATRP and FRP. *Macromolecules* **2010**, *43*, 4791−4797.
(36) Zhang, W.; Yuan, J.; Weiss, S.; Ye, X.; Li, C.; Müller, A. H. E. Telechelic Hybrid Poly(Acrylic Acid)s Containing Polyhedral Oligomeric Silsesquioxane (POSS) and Their Self-Assembly in Water. *Macromolecules* **2011**, *44*, 6891−6898.
(37) Roy, S. G.; Acharya, R.; Chatterji, U.; De, P. RAFT Polymerization of Methacrylates Containing a Tryptophan Moiety: Controlled Synthesis of Biocompatible Fluorescent Cationic Chiral Polymers with Smart pH-Responsiveness. *Polym. Chem.* **2013**, *4*, 1141−1152.
(38) Narayanan, A.; Bauri, K.; Ruidas, B.; Pradhan, G.; Banerjee, S.; De, P. Specific Counterion Repercussions on the Thermal, pH-Response, and Electrochemical Properties of Side-Chain Leucine Based Chiral Polyelectrolytes. *Langmuir* **2014**, *30*, 13430−13437.
(39) Deng, G.; Tang, C.; Li, F.; Jiang, H.; Chen, Y. Covalent Cross-Linked Polymer Gels with Reversible Sol−Gel Transition and Self-Healing Properties. *Macromolecules* **2010**, *43*, 1191−1194.
(40) Soliman, E. A.; El-Kousy, S. M.; Abd-Elbary, H. M.; Abou-Zeid, A. R. Low Molecular Weight Chitosan-Based Schiff Bases: Synthesis,

DOI: 10.1021/acsami.5b01272
ACS Appl. Mater. Interfaces 2015, 7, 8779−8788

Characterization and Antibacterial Activity. *Am. J. Food Technol.* **2013**, *8*, 17−30.
(41) Roy, S. G.; Bauri, K.; Pal, S.; Goswami, A.; Madras, G.; De, P. Synthesis, Characterization and Thermal Degradation of Dual Temperature- and pH-Sensitive RAFT-Made Copolymers of *N*,*N*-(dimethylamino)ethyl Methacrylate and Methyl Methacrylate. *Polym. Int.* **2013**, *62*, 463−473.
(42) Wang, Q.; Mynar, J. L.; Yoshida, M.; Lee, E.; Lee, M.; Okuro, K.; Kinbara, K.; Aida, T. High-Water-Content Mouldable Hydrogels by Mixing Clay and a Dendritic Molecular Binder. *Nature* **2010**, *463*, 339−343.
(43) Bairi, P.; Chakraborty, P.; Mondal, S.; Roy, B.; Nandi, A. K. A Thixotropic Supramolecular Hydrogel of Adenine and Riboflavin-5′-Phosphate Sodium Salt Showing Enhanced Fluorescence Properties. *Soft Matter* **2014**, *10*, 5114−5120.
(44) Saha, S.; Bachl, J.; Kundu, T.; Díaz, D. D.; Banerjee, R. Amino Acid-Based Multiresponsive Low-Molecular Weight Metallohydrogels with Load-Bearing and Rapid Self-Healing Abilities. *Chem. Commun.* **2014**, *50*, 3004−3006.
(45) Roy, S. G.; De, P. Swelling Properties of Amino Acid Containing Cross-Linked Polymeric Organogels and Their Respective Polyelectrolytic Hydrogels with pH and Salt Responsive Property. *Polymer* **2014**, *55*, 5425−5434.
(46) Roy, S. G.; Haldar, U.; De, P. Remarkable Swelling Capability of Amino Acid Based Cross-Linked Polymer Networks in Organic and Aqueous Medium. *ACS Appl. Mater. Interfaces* **2014**, *6*, 4233−4241.
(47) Yan, C.; Pochan, D. J. Rheological Properties of Peptide-Based Hydrogels for Biomedical and Other Applications. *Chem. Soc. Rev.* **2010**, *39*, 3528−3540.
(48) Guvendiren, M.; Lu, H. D.; Burdick, J. A. Shear-Thinning Hydrogels for Biomedical Applications. *Soft Matter* **2012**, *8*, 260−272.

DOI: 10.1021/acsami.5b01272
ACS Appl. Mater. Interfaces 2015, 7, 8779−8788